International Journal of Research in Engineering and Science (IJRES)
ISSN (Online): 2320-9364, ISSN (Print): 2320-9356
www.ijres.org Volume 6 Issue 5 ǁ May. 2018 ǁ PP.92-106

Study on surface integrity of Ti-6Al-4V machined by WEDM

Ranjan Kumar, Pallavi Parimita, Chandrabhanu Malla, Satyakam Acharya
S. Sarkar*

Department of Mechanical Engineering, NM Institute of Engineering and Technology,Bhubaneswar , Odisha
Department of Mechanical Engineering, Raajdhani Engineering College,Bhubaneswar,Odisha
Department of Mechanical Engineering,Aryan Institute of Engineering and Technology Bhubnaeswar , Odisha
Department of Mechanical Engineering,Capital Engineering College,Bhubaneswar,Odisha

ABSTRACT: *This paper focuses on investigating surface integrity of low-speed wire electrical discharge machining (LS-WEDM) in machining Ti-6Al-4V (TC4) by multiple cuts namely one main cut (MC) followed by trim cuts (TC). The machining parameter levels of multiple cuts and offsets were modified aimed at TC4 material, and the surface roughness of 0.67 μm was obtained after one MC and three TC. In addition, scanning electron microscopy (SEM) was used to observe the surface micro-structure, which is characterized by an uneven fusing struc-ture, spherical droplets, irregular droplets, craters, cracks, and micro-void; Moreover, it can be observed that cracks usually began with the edge of micro-voids, and the debris on the machined surface were deformed fragments due to the low thermal conductivity makes TC4 material be ejected or solid-ified before completely melting. Furthermore, the foreign el-ements of Cu and Zn were detected in the white layer by energy dispersive spectrograph (EDS) integrated in SEM; it also can be found that the crater edge has more Cu and Zn elements than crater center. The white layers were predomi-nantly nonuniform and discontinuous due to poor penetration hardening of TC4 material. After the third TC, the white layer.has become more continuous and the thickness was reduced to 2.7 μm, which was nearly invisible. The hardness of the white layer was almost the same as the base material. Finally, the blueviolet film was observed on the TC4 workpiece surface due to the electrolysis making the surface oxidation. By using X-ray diffraction (XRD), it is confirmed that TiO_2, Ti_2O_3, and TiO existed in the oxidation film. The technique and knowl-edge that this study proposed could provide a significant con-tribution to electrical discharge machining surface improvement.*

Keywords *Ti-6Al-4V, LS WEDM, Surface integrity*

I. INTRODUCTION

Titanium alloy possess many attractive properties like out-standing mechanical and thermal properties, excellent corro-sion resistance, and high strength to weight ratio, which makes it to be one of the most widely used materials for successful application in the aerospace, automotive, and biomedical in-dustries [1, 2]. But titanium alloy still has some weak attri-butes such as poor thermal conductivity and high chemical reactivity with tool materials, which will impair it machinabil-ity of conventional machining and make it to be one of the typical difficult-to-machine materials [3]. Low-speed wire electrical discharge machining (LS-WEDM) as an important method of nontraditional machining contributes a predomi-nant role in the tool making, automobile, and aerospace indus-tries, since it is capable of efficiently and automatically fabri-cating various parts of complex geometrical shapes and not restricted by the material properties such as strength, hardness, and toughness [4, 5]. Therefore, LS-WEDM can circumvent problems encountered in conventional machining methods and to be the best alternative to manufacture titanium alloy components and parts.

The thermal nature of the electrical discharge machining process provides significant advantages in machining difficult-to-machine materials but it also produces its own problem. During the electrical discharge machining, the work-piece surface is subjected to instantaneous high temperature (10000 ℃) and rapid cooling, which significantly affect the workpiece's micro-topography, chemical composition, metal-lographic structure, and surface physical properties. Moreover, the change in the machined surface will have a critical influence on the functional performance of the parts such as fatigue life, wear, and corrosion resistance, which has restricted LS-WEDM application in the aerospace industry [6]. Therefore, as an important method for precision machining of difficult-to-machine material, the surface quality im-provement of WEDM has attracted more research interests.

Shajan et al. [7] optimized surface characteristics of TC4 based on a Non-Dominated Sorting Genetic Algorithm (NSGA). Danial et al. [8] used response surface methodology to investigate the WEDM optimized setting of TC4 and found the pulse on time has the highest impact on surface roughness. Kuriachen et al. [9] used fuzzy modeling and PSO algorithm to optimize the machining parameters for surface roughness of WEDM for TC4. Pasam et al. [10] determined the optimal parameters for surface finish in WEDM of titanium alloys by Taguchi methodology. Caydas et al. [11] found that pulse off time had little influence on white layer thickness

(WLT), and the pulse time is the most significant factor. Vivek et al. [12] built an empirical modeling of process parameters of the WEDM using RSM, and the optimized values of cutting rate and surface roughness achieved through multiresponse opti-mization are 2.55 mm/min and 2.54 μm, respectively. Thomas et al. [13] investigated the effect of process parameters on the formation and characteristics of white layer in WEDM.

From the discussion above, it could be seen that many researchers have been devoting their efforts to improve the surface quality by parameters optimization and the experi-ments they conducted are single cut, but the most effective method to improve the surface quality is multiple cutting tech-nology. The electrical discharge machining equipment can provide optimal machining parameters for conventional ma-terials such as steel, copper, tungsten carbide, and so on. But until now, the existing electrical discharge machine system cannot provide the optimal machining parameters and multi-ple cutting strategies aimed at titanium alloy. In term of work-piece material, though TC4 is one of the most important tita-nium alloy widely used in the aviation and aerospace indus-tries, there are few previous investigations concerning all as-pects of the surface integrity of TC4 workpiece machined by LS-WEDM with multiple cuts. Therefore, this study is an attempt to investigate the surface integrity of TC4 material under multiple cuts using LS-WEDM.

II. EXPERIMENTAL PROCEDURES

2.1 Equipment and machining conditions

The experiments were carried on CA20 made by Beijing Agie Charmilles Industrial Electronics Co. Ltd. The machining schematic diagram is shown in Fig. 1; the brass wire with a diameter of 200 μm is drawn through a set of upper and lower guides. The wire does one-way movement in a low wire speed along the predetermined cutting trajectory, and the mechanical tensioning device is applied to maintain the wire in tension. The wire is independent of electrode wear, which differs from high speed wire electrical discharge machining (HS-WEDM); the TC4 material is eroded by a series of discrete sparks be-tween the workpiece and the brass wire separated by discharge gap; the discharge gap is precisely kept by the LS-WEDM control system. During the machining, the workpiece is im-merged in deionized water (dielectric fluid), which is contin-uously fed to the cutting zone to flush away the debris [14]. In the deionized water, the electrochemical reaction inevitably exists and the higher conductivity will exacerbate electro-chemical reaction. Therefore, the lower conductivity of 5 μs/ cm is set after combining with the actual processing condi-tions of the experiment equipment.

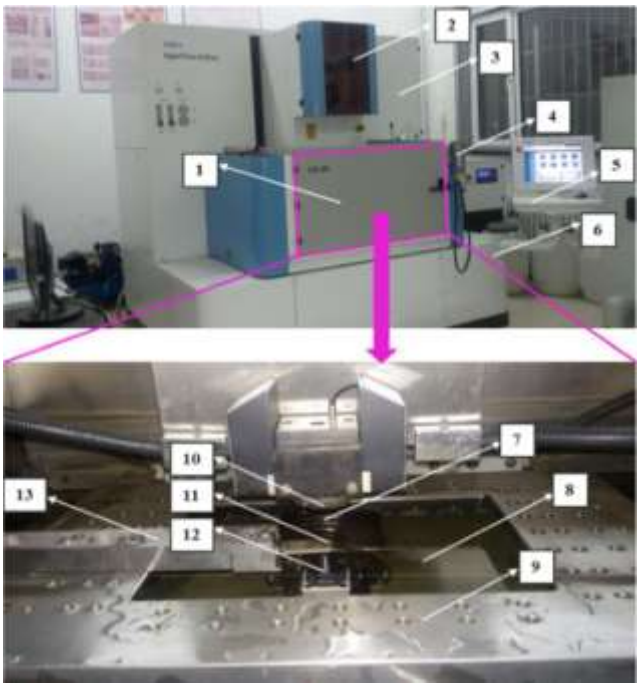

Fig. 1 LS-WEDM equipment used for experimentation. 1 fluid bath, 2 movement wire device, 3 electric cabinet, 4 operating handle, 5 manipulation platform, 6 water tank, 7 the brass wire, 8 deionized water, 9 workbench, 10 the upper guide, 11 TC4 workpiece, 12 the lower guide, 13 fixture

Table 1 Experimental conditions of TC4 by LS-WEDM

Parameters	Unit	Machining value
Brass diameter	mm	0.2
Workpiece material		TC4
Wire material		Brass
Polarity		Positive
Work fluid		Deionized water
Thickness of TC4	mm	5 ± 0.010
Cutting length	mm	6
Angel of cut		Vertical
Dielectric temperature	°C	25
Conductivity	μs/cm	5
Flux	L/min	4

Table 3 Material properties of TC4

Content	Values
Elastic modulus (GPa)	114
Melting point (°C)	1630
Electrical resistivity (μΩ.cm)	178
Thermal conductivity (W/m.K)	6.70
Density (g/cm^3)	4.04
Yield strength (kg/mm^2)	84.2
Tensile strength (kg/mm^2)	91.3
Elongation (%)	10
Poisson ratio	0.33

workpiece and the guide nozzle is 0.1 mm to reduce the wire vibration. Detailed processing conditions were shown in Table 1.

TC4 was taken as the work material and prepared with 5 mm × 20 mm × 25 mm in dimensions, the chemical compo-sition is given in the Table 2, and the properties of TC4 shown in the Table 3. The thickness of the workpiece greatly affects the working liquid inflow and outflow, debris ejection, deion-ization, and so on. If the thickness is too small, it will cause discharge concentration, surface burning, and be liable to cause wire breakage; if the thickness is too big, it will make the work fluid difficult to enter the discharge gap and lead to poor processing stability. Besides, the dimensions of 100 μm~10 mm are between macroscopic and microscopic, which has the extremely widespread application. Moreover, the thickness range of the experiment machine is from 5 to 80 mm. Therefore, the thickness of 5 mm was chosen after synthesizing the above various factors.

2.2 Experiment design

In the LS-WEDM process, multiple cutting is the most effec-tive method to improve the surface quality. The built-in data-base of the commercial WEDM machine can automatically select process parameters according to the material type and workpiece thickness. But titanium alloy is not yet a material in the database.
In this experiment, the MC was followed by three TC. In the MC, the highest discharge energy together with high

Table 2 Chemical composition of TC4 (wt %)

Composition	C	Fe	N	O
Weight percent	≤0.10	≤0.30	≤0.05	≤0.20
Composition	Al	V	H	Ti
Weight percent	5.5 ~ 6.8	3.5 ~ 4.5	≤0.015	Balance

flushing pressure and wire speed were applied for increasing the processing efficiency. Besides, the wire tension in the trim cuts should be higher than the main cut, this is due to the main cut is bilateral discharge and the discharge spark force on the wire electrode is symmetric, which has restrictions on the wire vibration and is beneficial to cut stably. But the trim cuts are unilateral discharge without symmetric restraint force, so the higher wire tension and lower discharge energy were applied in the TC1 (the first trim cut) to improve the dimensional accuracy. As for TC2 (the second trim cut) and TC3 (the third trim cut), the alternating pulse is set, which can make the average voltage to be zero by generating a negative voltage during pulse off time to counteract the positive voltage of pulse on time. In this way, the alternating pulse can make ions from deionized water is kept oscillated, neither towards brass nor towards the TC4 workpiece, which can effectively restrain the electrochemical corrosion and surface oxidation. The low thermal conductivity and low plasticity of titanium alloy ma-terial tend to cause wire breakage due to the high temperature during machining. Therefore, the machining parameter levels of multiple cuts and offsets (shown in 3.1) were modified in order to reduce the incidence of wire breakage and provide stable machining as given in Table 4.

Table 4 LS-WEDM machining parameters of multiple cuts

Parameters	Unit	MC	TC1	TC2	TC3
Peak current ($i^{\wedge}_e$)	A	320	230	110	40
Open voltage ($\hat{u}_i$)	V	136	85	68	51
Pulse on time (t_i)	μs	15	13	6	4
Pulse off time (t_O)	μs	25	25	25	25
Negative pulse	1	0	0	1	1
Positive pulse	1	1	1	1	1
Wire tension (F_w)	N	12	15	18	18
Wire speed (A_w)	mm/s	180	165	150	135
Feeding speed (V_s)	mm/min	0.01	0.01	7	4
Flushing pressure	bar	10	1	0.3	0.3
Offset	μm	195	149	122	110

Table 5 The offset value of carbide provided by machine system

Cut times	Offset (μm)				Increment (μm)
	1	2	3	4	
Main cut	123	158	183	195	—
Trim 1	—	112	137	149	46
Trim 2	—	—	110	122	37

Trim 3	—	—	—	110	12

III. RESULT AND DISCUSSION

3.1 Offset determination

The offset is crucial in the multiple cuts, which will determine the dimensional accuracy and surface quality. The smaller offset will make it difficult to remove or minimize the thermal damage by subsequent trim cuts and cannot achieve the pur-pose of multiple cutting. The larger offset will affect the ma-chining speed and wire vibration damping. Therefore, it is not conducive to reduce the surface roughness and enhance sur-face quality with larger or smaller offset. The offset is the distance from the wire center line to the machining surface, which is equal to the sum of the unilateral discharge gap and the radius of the brass wire.

The experiment material is titanium alloy and not carbide, the offset aimed at carbide material recommended from the built-in database of machine system shown in Table 5, which is unfit for titanium alloy. Therefore, the offset of titanium alloy should be modified one by one.

First, the single cut was conducted with the offset of 123 μm provided by built-in database. Then, the Kerf width was observed by VHX-1000E microscope and measurements were replicated at five different locations shown in Fig. 2a. Furthermore, the three-dimensional surface spacing method was taken for measuring accurately demonstrated in Fig. 2b. The average result is 264 μm, which is different from the theory value of 246 μm (2 × 123 μm = 246 μm). Due to the single cut is bilateral discharge and the brass wire diameter is 200 μm, so the actual unilateral discharge gap of 23 μm can be

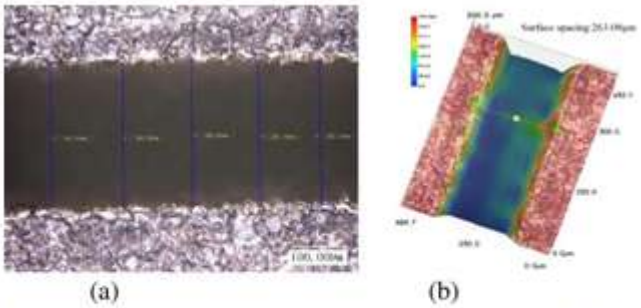

(a) (b)

Fig. 2 Kerf width of TC4. a Two-dimensional measurement. b Three-dimensional measurement

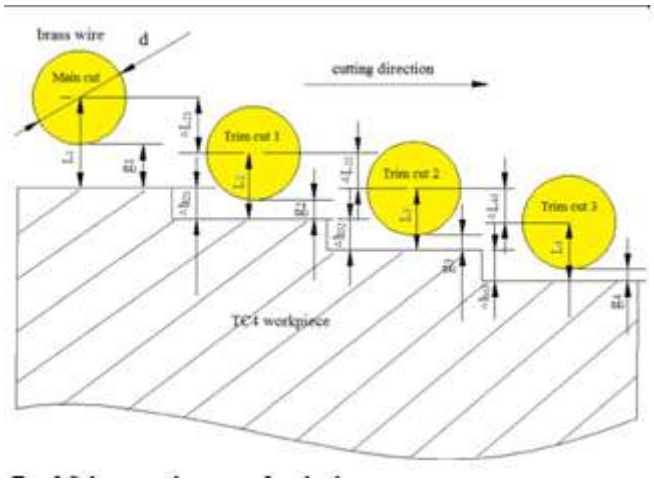

Fig. 3 Schematic diagram of multiple cuts

calculated. In order to obtain high dimensional accuracy, the offset of 123 μm provided by the database must be modified to 132 μm.

Equations (1) and (2) can be obtained according to the schematic diagram of four cuts shown in Fig. 3. The height difference of the adjacent two cuts was measured by VHX-1000E microscope shown in Fig. 4, and the results were dem-onstrated in Table 6.

L_{n-1} is the wire offset of the (n-1)th cut (μm); L_n is the wire offset of the nth cut (μm), and n = 2,3,4,5.

$\triangle h_{n(n-1)}$ is the height difference after two cuts (μm); $\triangle L_{n(n-1)}$ is offset increment of adjacent cuts (μm); d is the brass wire diameter (μm); and g_n is the unilateral discharge gap of the nth cut (μm).

The unilateral discharge gap values respectively were 23, 18, 7, and 3 μm from MC to TC3, which were calculated according to Equations (1) and (2) and the measurement of Table 6. In order to ensure the final dimensional accuracy, the offset of the third trim was 103 μm, which was the sum of the third unilateral discharge gap and the radius of the brass wire (200/2 + 3 = 103 μm). The offset increment of adjacent cuts

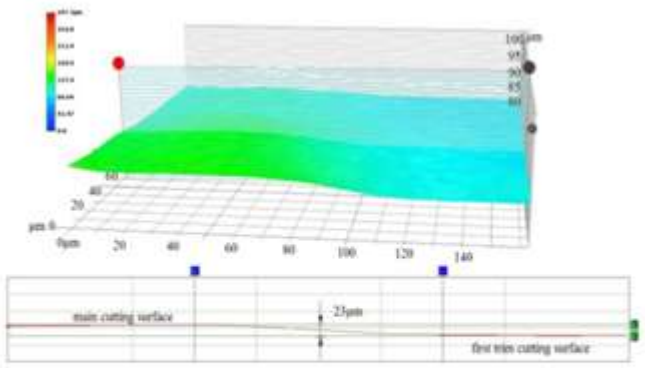

Fig. 4 Measurement of height difference of first and second cuts

Table 6 The height difference of adjacent cuts

Height difference	$\triangle h_{21}$	$\triangle h_{32}$	$\triangle h_{43}$
Value (μm)	32	26	8

were, in the order, 36, 25, and 10 μm after taking the machin-ing allowance and all cutting discharge gap into consideration. Therefore, the offset from the main cut to the third trim cut respectively were 174, 138, 113, and 103 μm. The offsets of multiple cuts for TC4 of 5 mm thickness were listed in Table 7. Experimental results indicated that the machining process can be conducted stably, and the surface quality can be greatly improved according to the multiple cutting condi-tions given in Table 4 and the offset given in Table 7.

3.2 Surface roughness

T h e n o n - c o n t a c t 3 D s ur f a c e p r o f i l o m e t e r w i t h 300 μm × 300 μm measured range was used to observe the machined surface and measure the surface roughness, shown in Fig. 5. The surface roughness parameters are tabulated in Table 8. The target Sa (surface roughness) of four cuts for carbide is 0.9~1.0 μm; nevertheless, the Sa of 0.67 μm was produced due to the fact that machining parameters and offsets of multiple cuts have been modified for TC4 material.

The surface topography of MC and TC are respectively shown in Figs. 6, 7, 8, and 9. It can be seen that numerous and nondirectional craters distributed randomly on the sur-face. Fig. 6a shows the crater is lager and deeper due to the high discharge energy and the height range of the z axis is −7.5~5 μm. The crater depth is reduced evidently with the increased cutting times as Figs. 7a and 8a show, and the height range of the z axis has reduced to −4~2 μm after the third trim cut shown in Fig. 9a.

Figures 6b, 7b, 8b, and 9b detailed the cross-sectional con-tours of MC and TC; the wave peaks and valleys were becom-ing more intensive and the distance of adjacent wave peaks was becoming narrower; therefore, it can be deduced that the distribution of craters becomes dense and uniform, and craters were becoming smaller both in width and depth. Moreover,

Table 7 The offset value of TC4 after modifying

Cut times	Offset (μm)				Increment (μm)
	1	2	3	4	
Main cut	132	149	165	174	–
Trim 1	–	113	129	138	36
Trim 2	–	–	104	113	25
Trim 3	–	–	–	103	10

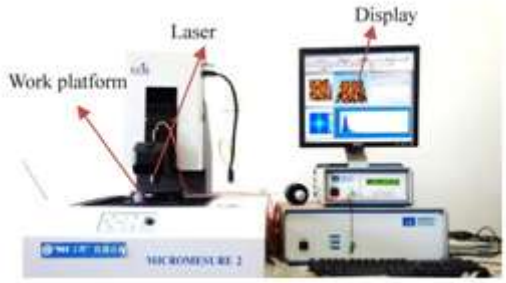

Fig. 5 3D surface profilometer

the sectional contour height has reached nanometer level after TC3, shown in Fig. 9b.

3.3 Surface microstructure

The LS-WEDMed workpieces were prepared with ultrasonic cleaning for 10 min followed by air drying, and then, the surface microstructure were observed usingJSM-7001F scan-ning electron microscope (SEM). From Fig. 10a, b, c, d, it can be observed that the surface is characterized by an uneven fusing structure, spherical droplets, irregular droplets, craters, cracks, and micro-voids, which is different from the mechan-ical machining surface. The irregular droplets are due to the melting material has not been thrown away and solidified on the machined surface. The spherical droplets are due to the vaporized material, which are cooled by the deionized water and re-solidified on the machined surface.

The voids can be attributed to the gas bubbles expelled from the molten material during solidification. The voids are small both in main and trim cuts, shown in Fig. 10, this is because the deionized water' cooling rate is large and the bubbles do not have enough time to grow up before the ma-terial solidification. In addition, it also can be found that cracks usually began with the edge of micro-voids, shown in Fig. 11. On the one hand, the micro-voids can reduce the workpiece surface tensile strength, which will increase the possibility of cracks formation. On the other hand, the micro-voids will change the curvature radius of the workpiece surface, which increases the cooling rate around micro-voids and then results in the increase of the material's internal tensile stress.

The cracks are related to the rapid cooling and the higher thermal stresses exceeding the fracture strength. As for TC4

Table 8 3D surface roughness parameters

Name	Unit	Description	MC	TC1	TC2	TC3
Sa	μm	Arithmetic mean height	1.74	1.40	1.25	0.67
Sq	μm	root mean square roughness	2.33	1.81	1.58	0.85
Sy	μm	Maximum height	22.2	17.7	13.8	7.34
Sz	μm	Maximum peak height	16.9	16.7	12.0	6.99

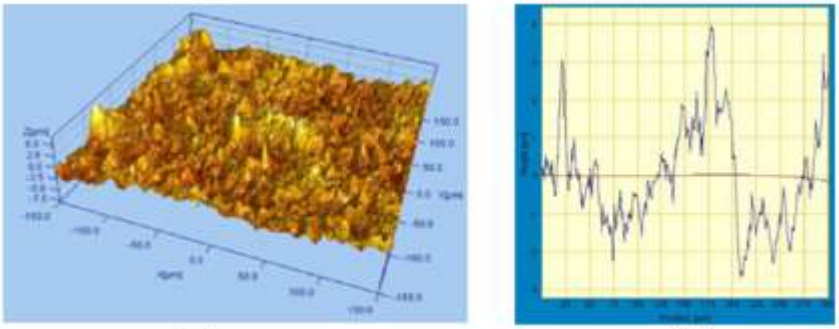

(a) (b)

Fig. 6 a Surface topography of MC. b Cross-sectional contour

materials, the cracks not only formed in the main cut but also in all trim cuts, which was different from IN718 without microcracks in the trim cuts [15]. The thermal conductivity has the most significant effect on cracks formation. TC4 ma-terial with low thermal conductivity cannot quickly conduct heat away, which will produce more cracks, as shown in Fig. 10a, b, c. Besides, the cracks were gradually reduced after the more trim cuts passing with low discharge energy. From Fig. 10d, it can be seen that the cracks are nearly invisible after TC3.

In the MC, the highest discharge energy makes most of molten material ejected but only a small part of ejected mate-rial was flushed away by the deionized water and most molten material was re-solidified on the surface as Fig. 10a. From Figs. 10b, c, d, it can be observed that the debris obviously reduced and many overlapped craters appeared on the surface. This is due to most of the molten TC4 material stayed on the surface and not splashed; thus, the craters can be found in the trim cuts.

Meanwhile, the debris on the machined TC4 speci-men surface was mainly deformed fragments shown in Fig. 12, which differed from steel with spherical debris [16]. This is due to the low thermal conductivity and high melting point of TC4 material makes it be ejected or solidified before completely melting. Besides, it can be found that the thermal stripping is another material removal mechanism except melting and evaporation of LS-WEDM for TC4. In Fig. 12, the deep cracks are

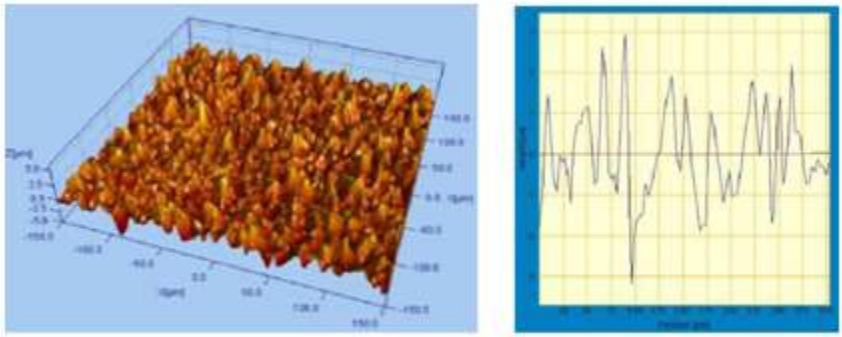

(a) (b)

Fig. 7 a Surface topography of TC1. b Cross-sectional contour

formed on the surface and material is stripped layer by layer, which is like the rock fault. It is suggested that TC4 material is ejected by some kind of mechani-cal force, namely, thermal stress. Thermal stress gener-ates from the uneven internal heating of TC4 material caused by volume heat source. In the MC, the high discharge energy and the poor thermal conductivity make the internal thermal stress of TC4 material greater than the grain boundary force, and then the whole grain would be separated from the TC4 materials, which all result in producing the thermal stripping material re-moval mechanism.

Besides, an energy dispersive spectrograph (EDS) as-sociated with the SEM was also used to investigate the elements present in a single discharge crater shown in Fig. 13a, and the EDS spectra of the crater center and edge were respectively shown in Fig. 13b, c. The for-eign elements of Cu and Zn were detected, which mi-grated from the brass wire. The amount of Cu deposi-tion is higher than the Zn element; this is due to zinc has lower melting and evaporation (419.5 °C) compared with Cu (1084.62 °C), so Zn is easier to be completely evaporated during machining. Besides, the proportion of Zn is much less than Cu in the brass wire. It

also can be observed that the crater edge has more Cu and Zn elements than the crater center, since the diffusion of Cu and Zn elements is rapid during the craters formation.

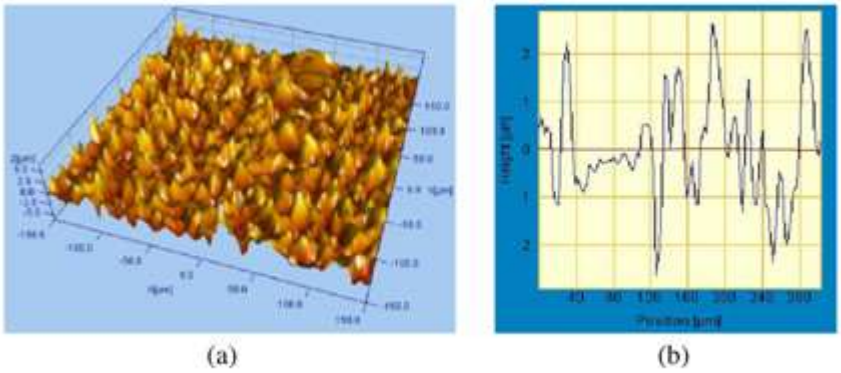

Fig. 8 a Surface topography of TC2. b Cross-sectional contour

3.4 The white layer

In order to observe the white layer using SEM, the TC4 spec-imens were grinded with 80–3000 mesh sandpaper after hav-ing been embedded in resin; then, the grinded surfaces were cleaned and polished with polishing paste. Finally, all pre-pared specimens were immersed in an etchant composed of 2 ml hydrofluoric acid, 10 ml nitric acid, and 88 ml water for 10 s. The cross-sectional micrographs of TC4 specimens after main and trim cuttings were measured by VHX-1000E micro-scope shown in Fig. 14. It can be found that the white layers were predominantly nonuniform and discontinuous due to poor penetration hardening of the TC4 material. With the cut-ting times increased, the white layer thickness was gradually decreased and the white layer has become more continuous. Therefore, it is evident that the thermal damage can be mini-mized by multiple cuts.

The finishing surface after TC3 was observed and measured by metallographic microscope shown in Fig. 15. It can be seen that the white layer thickness has reduced to 2.7 μm, which was nearly invisible. It is confirmed that the lower pulse discharge energy togeth-er with proper offset can effectively remove the previ-ous recast layer generated in the rough cut stage. Besides, three distinguished layers were observed, shown in Fig. 15. The upper layer is white through metallographic microscope, so the layer is termed as the white layer. The white layer is formed by molten

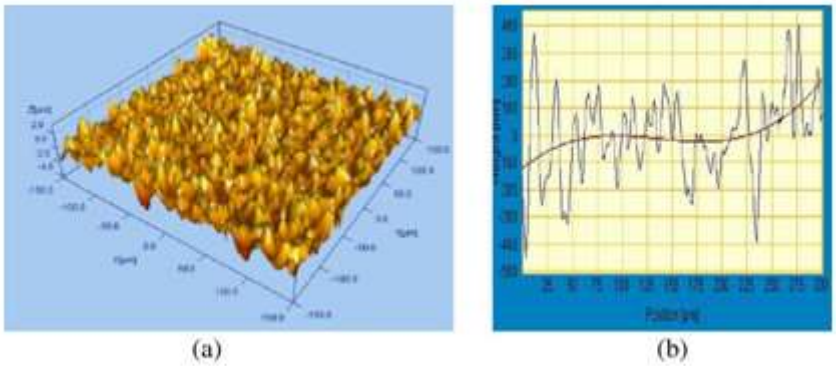

Fig. 9 a Surface topography of TC3. b Cross-sectional contour

metal which is not flushed away by the dielectric and re-solidifies on the TC4 workpiece surface during cooling [17]. The LS-WEDM process is similar to water quenching due to its extreme short discharge time, high machining temperature, and deionized water as work fluid, which will make the grain extremely small and even reach nanometer level in the white layer. In order to observe the nanometer grains, the white layer after TC3 was observed by SEM with 20000 times shown in Fig. 16. Furthermore, the heat-affected layer is below the white layer, which undergoes a thermal effect but not be molten. The heat-affected zone appeared as grain refinement phenomenon compared with the base materi-al as Fig. 15 show. As for the steel, the heated zone consists of

several layers including the hardened layer and annealed layer, but for the TC4 material, this phe-nomena cannot be found in this experiment; this is due to these layers' formation mainly depends on the pro-cess conditions and workpiece properties like thermal conductivity and chemical composition [18].

The microhardness test has been performed by using the microhardness tester with a load (100 mN) and a micro-diamond imprint. The microhardness was measured from the edge to the matrix along the cross-section. The depth profile of hardness of specimens formed by MC and TC were shown in Fig. 17. Results suggest that the hardness of the white layer is almost the same as the base material, which reflects the ex-tremely low white layer thickness.

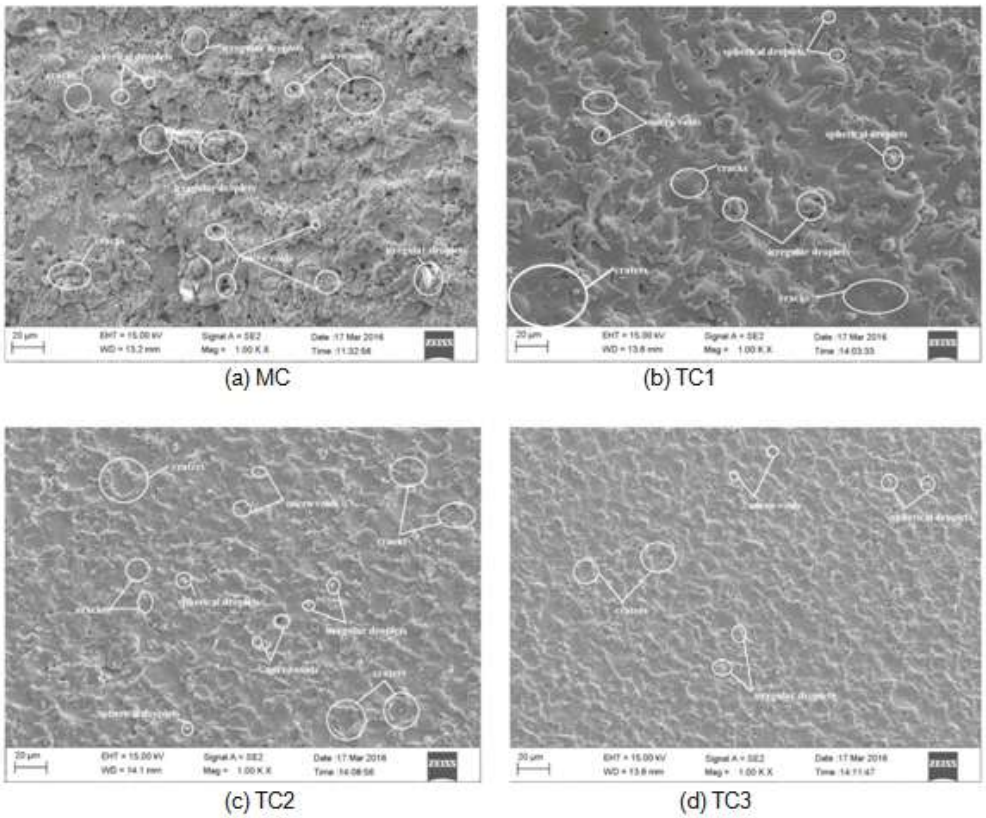

Fig. 10 Surface microstructure of multiple cuts on TC4

3.5 Surface oxidation

The machined surfaces of main and trim cuts are respectively observed using VHX-1000E microscope with 500 times high power lens, shown in Fig. 18. The surface is becoming smoother from MC to TC3, and the surface profile height from MC to TC are followed by 75.62, 56.38, 29.29, and 17.01 μm, which are gradually decreased. Besides, in Fig. 18a, it can be found that a large amount of copper at-tached on the surface of MC due to the high discharge energy exacerbated the metal transfer phenomenon shown, and this phenomenon is dramatically improved by the trim cuts;

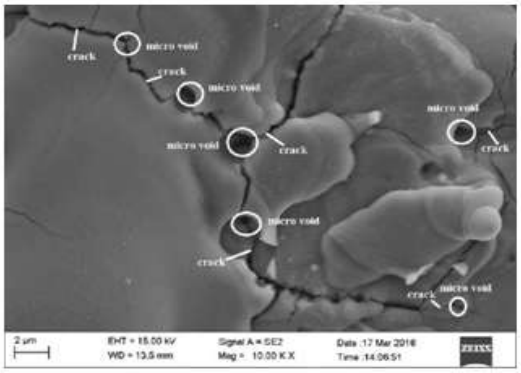

Fig. 11 The cracks near micro-voids

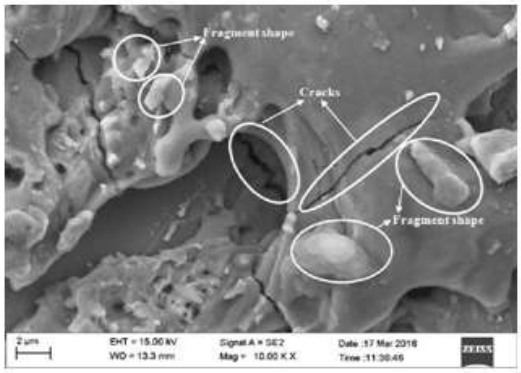

Fig. 12 The fragment shape debris of MC

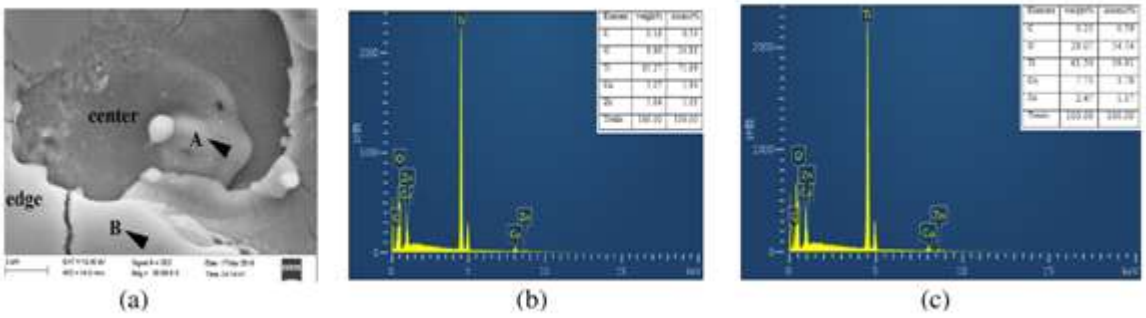

Fig. 13 a Elements analysis of a single discharge crater of TC3. b EDS spectra of position A. c EDS spectra of position B

Moreover, it also can be found that the blueviolet film formed on the surface after TC1 as shown in Fig. 18b; this is due to the electrolysis can make the oxidation film form on the TC4 workpiece surface.

Deionized water is a weak electrolyte, which will acceler-ate ionization and bring electrolytic reaction under the action of the electric field. For TC4 workpieces: $2OH^{-}$-2e = $1/2O_2$ + H_2O and gives out oxygen; for the brass wire: $2H^{+}$+2e = H_2, and gives out hydrogen. In addition, the high temperature of LS-WEDM during machining will make the deionized water in the plasma channel occur thermal dissociation, namely, H_2O = $2H^{+}$+$1/2O_2$ + $2e^{-}$, $2H^{+}$+$2e^{-}$ = $2H_2$; therefore, the elec-trons, OH^{-} ions and H^{+} ions respectively do directional move-ment to the cathode and anode under the action of the electric field.

Moreover, the leakage current produced in no-load or be-fore discharge breakdown will flow between the brass wire and workpiece, which make titanium atoms lose electrons and react with oxygen, and then generate titanium oxides such as Ti_2O_3, TiO_2, and TiO. These oxides will attach on the work-piece surface and form oxidation film. The oxidation film will make incident and reflected rays produce interference phe-nomenon and present colors. Figure 19 showed the XRD pat-terns, and it can be found that TiO_2, Ti_2O_3, and TiO existed in the oxidation film, which verified the above analysis.

The blueviolet oxidation film has the characteristics of a large resistance, poor electrical conductivity, and high melting point; it will prevent TC4 material remov-al rate and tend to cause short-circuit, thus affecting machining efficiency and stability. In order to suppress the formation of oxidation film and reduce electrochem-ical effect on the surface, two methods are put forward: one is using oil dielectric fluid and the other one is using alternating pulse. If the dielectric fluid is oil, the poor thermal conductivity of TC4 make the heat of discharge gap not easy to eliminate and result in arc discharge, which effect the machining stability; fur-thermore, titanium carbide will generate in the machin-ing process with high melting point and not easy to corrode, which will affect machining efficiency. Based on the above consideration, the alternating pulse was applied in TC2 and TC3, which can make the average voltage to be zero and make ions in the deionized wa-ter oscillated and neither towards the brass nor TC4 workpiece, thus the electrochemical corrosion and sur-face oxidation can be weaken. From Fig. 18c, the blue oxidation film was significantly reduced after TC2. After the TC3, the surface was greatly enhanced and the blueviolet oxidation film had disappeared complete-ly as shown in Fig. 18d.

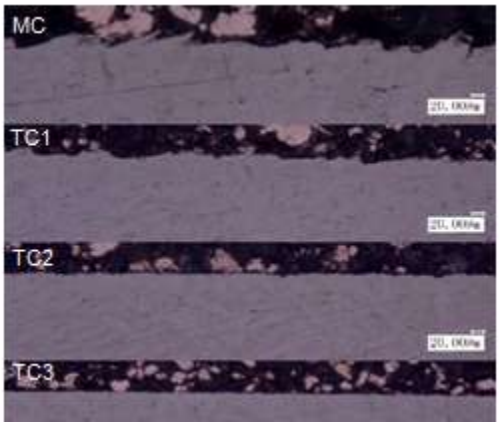

Fig. 14 The cross-sectional micrographs showing the white layer after TC3

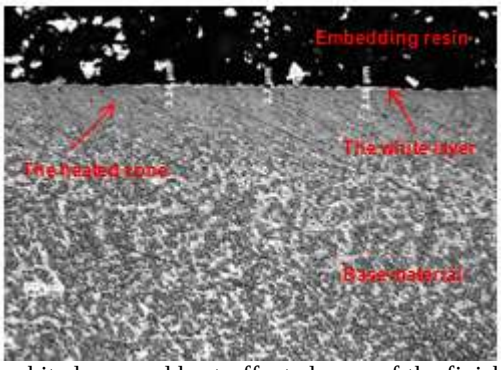

Fig. 15 The white layer and heat-affected zone of the finishing surface

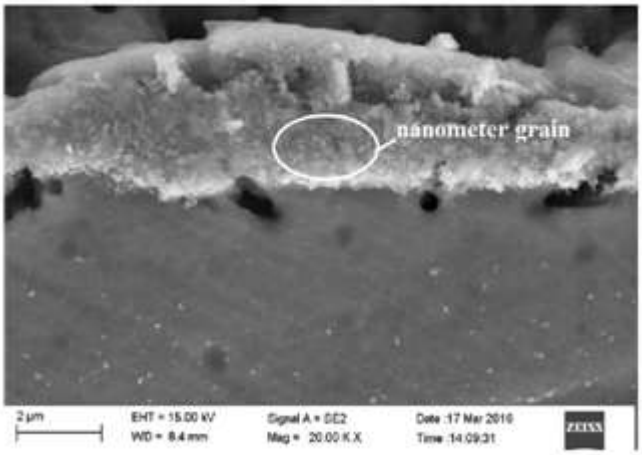

Fig. 16 The nanometer grains distributed on the white layer

IV. CONCLUSIONS

The following conclusions can be drawn from this experimen-tal research:

1. The machining parameters and offsets for multiple cuts are developed aimed at TC4 material. The surface rough-ness of 0.67 μm is obtained, and the sectional contour height has reached a nanometer level after one main and three trim cuts, which is superior to the target surface roughness (0.9~1.0 μm) of four cuts in the built-in data-base for carbide.

The experiment results show that the debris on the ma-chined TC4 specimen surface is mainly deformed frag-ments due to the low thermal conductivity and high melt-ing point of TC4 material makes it be ejected or solidified before completely melting; thermal stripping is another material removal mechanism except melting and evapo-ration of LS-WEDM for TC4; the cracks formed both in the main and trim cuts is due to the low thermal conduc-tivity of TC4 material; the voids are small both in the main and trim cuts due to the large cooling rate of deionized water, and the bubbles do not have enough time to grow up before the material solidification; the cracks usually begin with the edge of micro-voids due to they can reduce the workpiece surface tensile strength and change the cur-vature radius; the foreign elements of Cu and Zn can be detected on the machined surface, which are migrated from the brass wire, and the amount of Cu deposition is higher than Zn; moreover, the crater edge has more Cu and Zn elements than crater center.

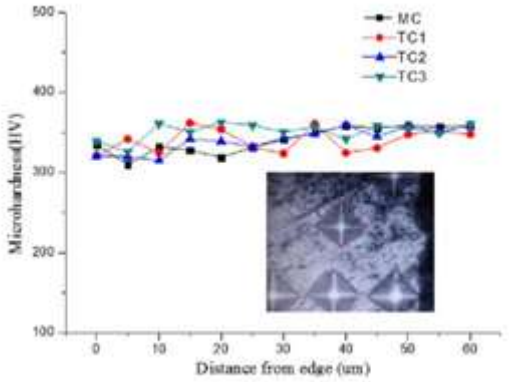

Fig. 17 Micro hardness results after multiple cuts

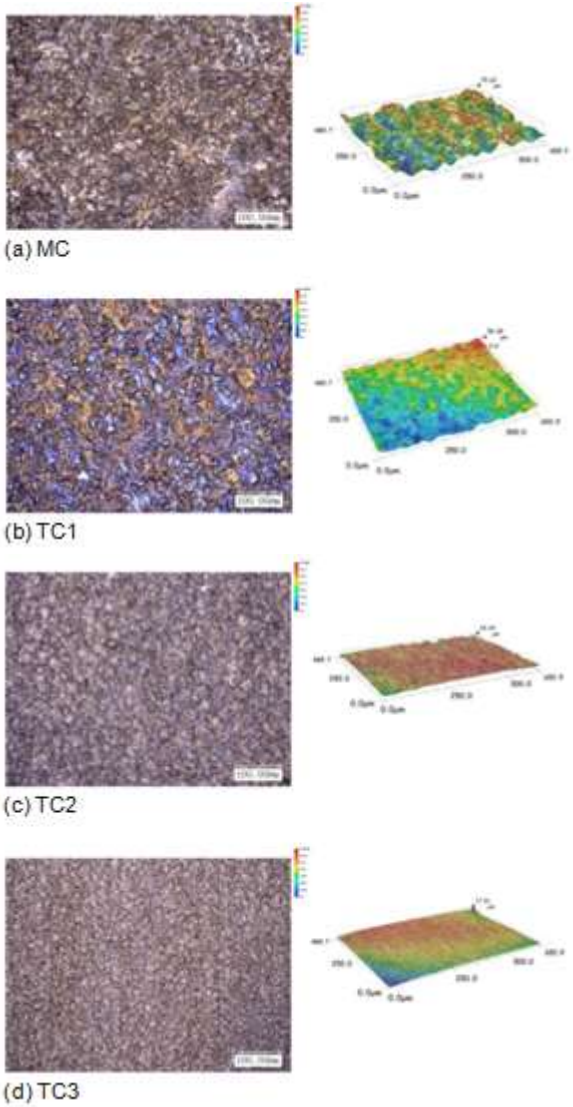

Fig. 18 The surface observed under VHX-1000E microscope

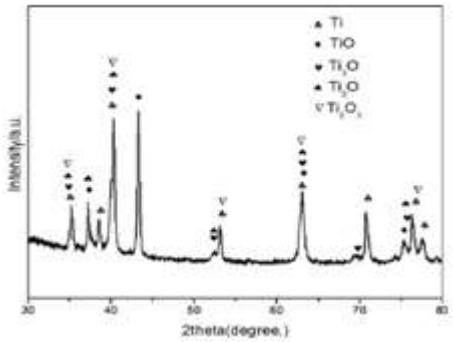

Fig. 19 The XRD patterns of WEDMed surface of TC4

The white layers of TC4 material are predominantly non-uniform and discontinuous due to its poor penetration hardening. After the third trim cut, the white layer has become more continuous and its thickness has reduced to 2.7 μm, which is nearly invisible; the heat-affected zone appeared as grain refinement phenomenon; nanome-ter grains are found on the white layer due to the extreme short discharge time and high machining temperature like the quenching; the hardness of the white layer and heated zone is almost same as the base material.

3. The blueviolet oxidation film can be observed on the TC4 workpiece surface due to the high temperature and elec-trochemistry make titanium react with oxygen. The XRD patterns have verified the existence of TiO_2, Ti_2O_3, and TiO in the blueviolet oxidation film. The electrochemical corrosion and surface oxidation can be weakened by ap-plying the alternating pulse in the trim cuts, and the blueviolet oxidation film has disappeared completely after the third trim cut.

REFERENCES

[1]. Mychal-Drew M, Jahan MP (2015) Micro-EDM machinability of difficult-to-cut Ti-6Al-4V against soft brass. Int J Adv Manuf Technol 81:1345–1361

[2]. Tiwary AP, Pradhan BB, Bhattacharyya B (2015) Study on the influence of micro-EDM process parameters during machining of Ti-6Al-4V superalloy. Int J Adv Manuf Technol 76:151–160

[3]. Kuriachen B, Alwin V, Somashekhar KP, Panda S, Mathew J (2015) Three-dimensional numerical simulation of microelectric discharge machining of Ti-6Al-4V. Int J Adv Manuf Technol 79: 147–160

[4]. Ikram A et al (2013) Parametric optimization for surface roughness, Kerf and MRR in wire electrical discharge machining (WEDM) using Taguchi design of experiment. J Mech Sci Technol 27(7): 2133–2141

[5]. Wang XZ, Liu ZD, Xue RY, Tian ZJ, Huang YH (2014) Research on the influence of dielectric characteristics on the EDM of titanium alloy. Int J Adv Manuf Technol 72(5-8):979–987

[6]. Hascalik A, Caydas U (2007) Electrical discharge machining of titanium alloy (Ti-6Al-4V). Appl Surf Sci 253:9007–9016

[7]. Shajan K, Shunmugam MS (2004) Characteristics of wire-electro discharge machined Ti6Al4V surface. Mater Lett 58:2231–2237

[8]. Ghodsiyeh D, Abolfazl G, Izman S (2014) Multi-objective process optimization of wire electrical discharge machining based on re-sponse surface methodology. J Braz Soc Mech Sci Eng 36:301–313

[9]. Kuriachen B, Somashekhar KP, Jose M (2015) Multiresponse op-timization of micro-wire electrical discharge machining process. Int J Adv Manuf Technol 76:91–104

[10]. Pasam VK, Battula SB, Madar VP, Swapna M (2010) Optimizing surface finish in WEDM using the Taguchi parameter design meth-od. J Braz Soc Mech Sci Eng 49:155–166

[11]. Caydas U, Ahmet H (2007) Modeling and analysis of electrode wear and white layer thickness in die-sinking EDM process through response surface methodology. Int J Adv Manuf Technol 38(11-12): 1148–1156

[12]. Aggarwal V, Khangura SS, Garg RK (2015) Parametric modeling and optimization for wire electrical discharge machining of Inconel 718 using response surface methodology. Int J Adv Manuf Technol 79:31–47

[13]. Newton TR, Melkote SN, Watkins TR et al (2009) Investigation of the effect of process parameters on the formation and characteristics of white layer in wire-EDM of Inconel 718. Mater Sci Eng, A 513-514:208–215

[14]. Mahapatra SS, Patnaik A (2007) Optimization of wire electrical discharge machining (WEDM) process parameters using Taguchi method. Int J Adv Manuf Technol 34:911–925

[15]. Li L, Wei XT, Li ZY (2014) Surface integrity evolution and ma-chining efficiency analysis of W-EDM of nickel-based alloy. Appl Surf Sci 313:138–143

[16]. Wang ZL, Chi GX, Di SC, Zhao WS (2000) Micro ultrasonic EDM of deep small holes in titanium alloys. Acta Arm Amentarii 21(4): 343–349

[17]. Patel KM, Pandey PM, Venkateswara Rao P (2009) Surface integ-rity and material removal mechanisms associated with the EDM of Al_2O_3 ceramic composite. Int Journal of Refractory Metals and Hard Materials 27:892–899

[18]. Bleys P, Kruth JP, Lauwers B, Schacht B, Balasubramanian V, Froyen L, Van HJ (2006) Surface and sub-surface quality of steel after EDM. Adv Eng Mater 8(1-2):15–25